

On the Sensitivity of Multiple-Scattering Calculations to the Single-Scattering Phase Function

H. B. HOWELL

Naval Research Laboratory, Washington, D. C.

(Manuscript received 23 April 1968, in revised form 8 July 1968)

ABSTRACT

Results of multiple-scattering calculations of diffuse reflection and diffuse transmission from scattering layers of different particle size and/or index of refraction are presented. Comparison of the results for each scattering model indicates the extent to which earlier calculations (for one cloud model) are generally applicable.

1. Introduction

In a recent paper (Twomey *et al.*, 1967) results of some multiple-scattering calculations for cloud layers were presented. These results included the diffuse reflection and diffuse transmission for assumed cloud models for a range of optical depths. The single-scattering phase functions used in all those models were

computed for poly-dispersions of spherical water droplets (index of refraction=1.33). Some indication was given as to the variation of certain calculated quantities with respect to change in the droplet-size distribution, but only the extreme values (an envelope of curves) were given, without giving explicitly the curves corresponding to various cloud models. Since the time of publication of those results some interest has been expressed as to their general applicability to scattering media which consist of dielectric spheres of different sizes and/or different indices of refraction. The purpose

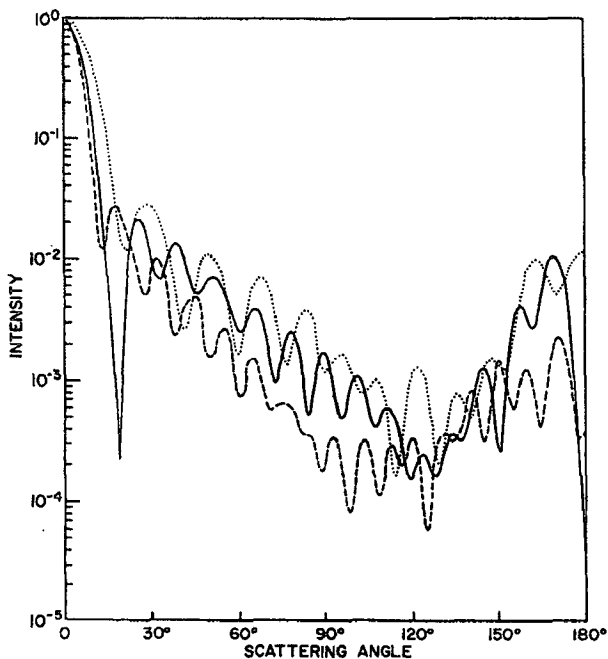


FIG. 1. Single-scattering Mie phase functions for three scattering models: 1) A Gaussian size distribution of water droplets (index of refraction=1.33) with a mean radius of 2μ , and a standard deviation of about 0.5μ . The mean size parameter is approximately 17 for incident radiation of wavelength 0.76μ (dashed curve). 2) A monodisperse aerosol of size parameter 16 and index of refraction 1.50 (solid curve). 3) A monodisperse aerosol of size parameter 11 and index of refraction 1.50 (dotted curve).

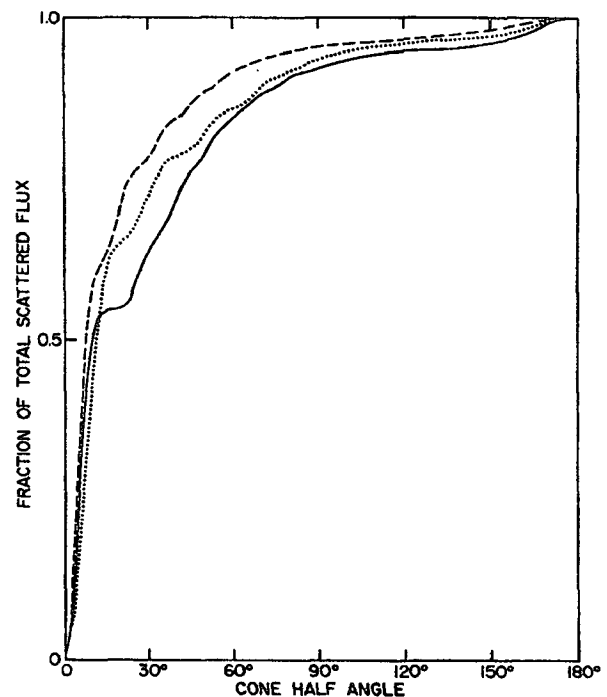


FIG. 2. The fraction of total scattered flux contained in a cone of half angle Θ around the forward (0°) direction for the three scattering models described in the legend of Fig. 1.

of this work is to present some results which show changes in calculated quantities resulting from changes in the size and index of refraction of the scattering particles. Except for the different single-scattering phase functions employed, the computational procedure used here is identical to that used in the work referred to above.

2. The models

The scattering-layer models used in this work are:

MODEL 1. A Gaussian size distribution of water droplets (index of refraction=1.33) with a mean radius of 2μ , and a standard deviation of the radii of about 0.5μ . The wavelength of incident light was 0.76μ , so that the mean size parameter α was approximately 17 ($\alpha = 2\pi r/\lambda$, where r is the radius of the scattering

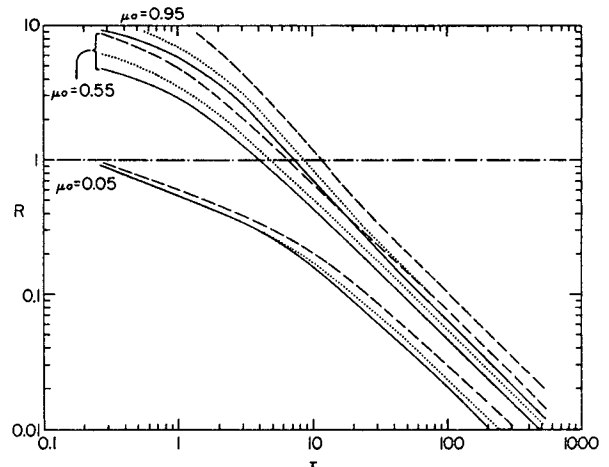


FIG. 3. The ratio of the diffuse radiation scattered downward to that scattered upward by a scattering layer of optical thickness τ , for the three scattering models described in the legend to Fig. 1.

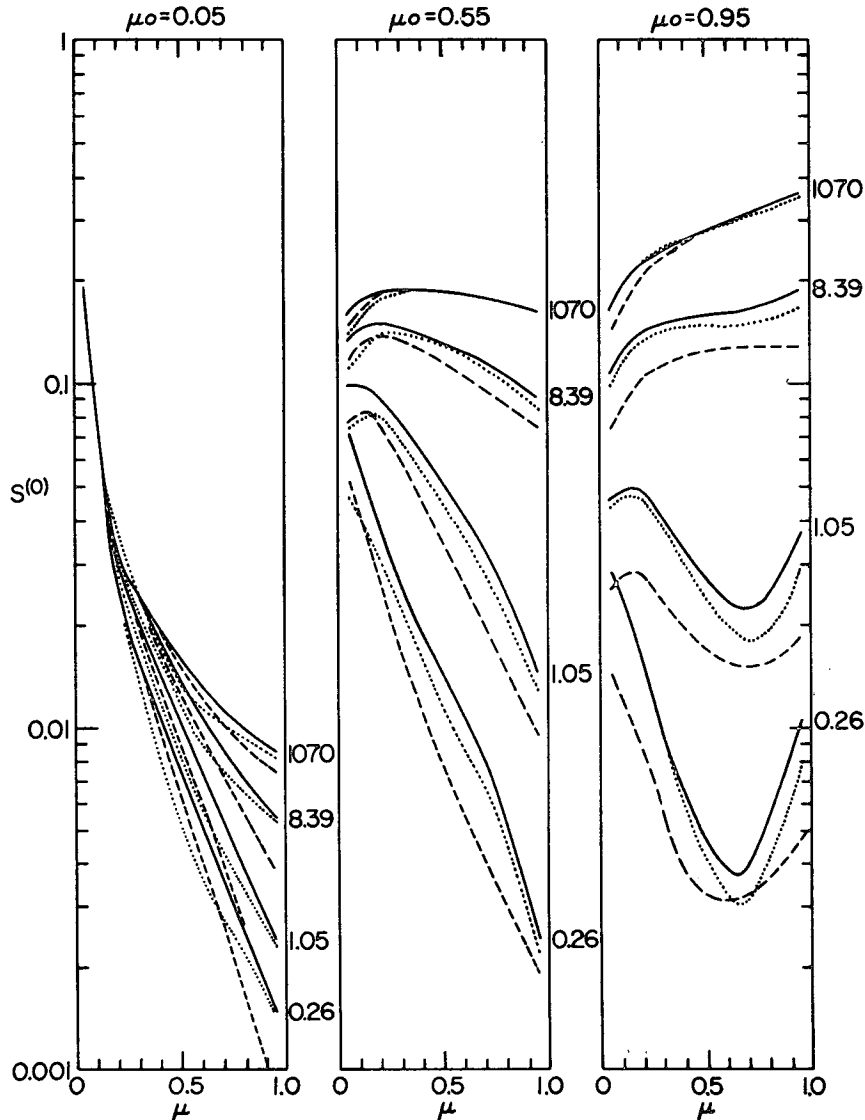


FIG. 4. Diffuse reflection $S^{(0)}$ vs μ for the three scattering models described in the legend to Fig. 1. Optical thickness is indicated beside each set of curves.

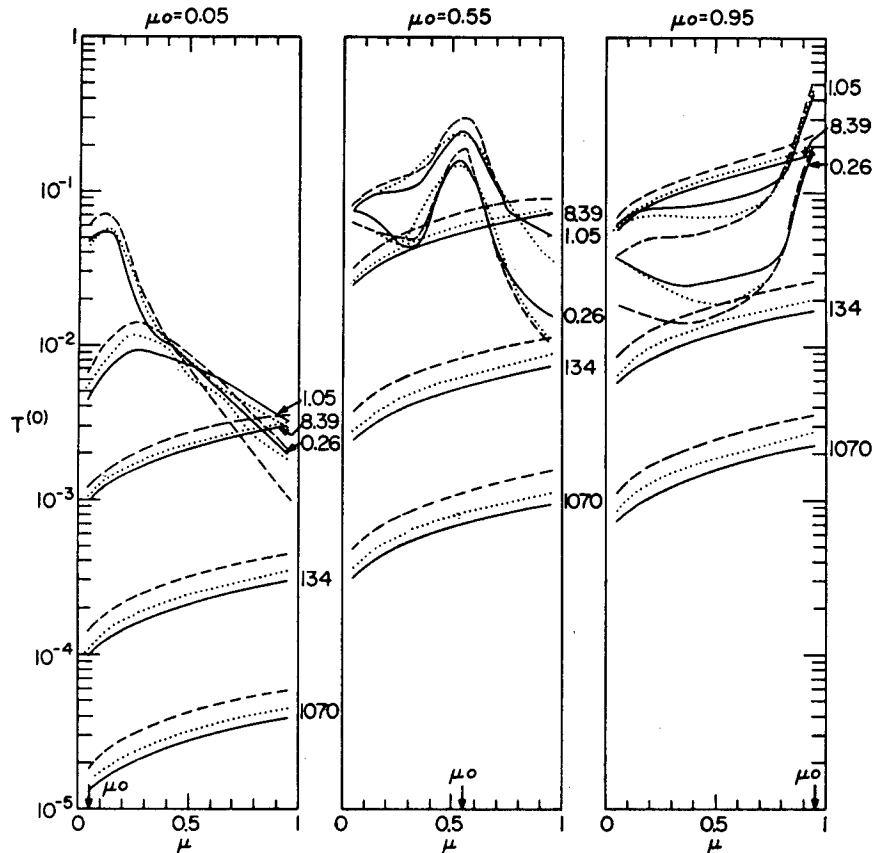


FIG. 5. Diffuse transmission $T^{(0)}$ vs μ for the three scattering models described in the legend to Fig. 1. Optical thickness is indicated beside each set of curves.

particle and λ the wavelength of the incident radiation).

MODEL 2. A monodisperse aerosol of size parameter 16 and an index of refraction 1.50.

MODEL 3. A monodisperse aerosol of size parameter 11 and an index of refraction 1.50.

In all three cases the albedo of single scattering was taken as unity (i.e., no absorption).

3. Terminology

For a complete explanation of the terminology used here the reader should consult Twomey *et al.* (1966, 1967). Briefly, $S^{(0)}$ and $T^{(0)}$ relate incident (downward) intensity to the diffusely reflected intensity and diffusely transmitted intensity, respectively, for a number of incident and emergent directions. These directions are described by the cosine μ of the acute angle between the intensity vector and the normal to the scattering layer. A zero subscript (e.g., μ_0) identifies the incident direction. The zero superscript indicates that $S^{(0)}$ and $T^{(0)}$ are

the constant terms in a Fourier expansion of S and T , i.e., they are averages over azimuth.

4. Results of calculations

The single-scattering phase functions, normalized to unit intensity in the forward (0°) direction, are shown in Fig. 1. Fig. 2 illustrates the forward-to-backward asymmetry of the phase functions in terms of the fraction of total scattered flux contained in a cone of half-angle Θ around the forward direction. Model 1 has consistently the *most*, and model 2 the *least* (for $\Theta > 15^\circ$), forward-peaked phase function. This feature of the phase function for models 1 and 2 will be of interest in the consideration of the figures which follow.

The ratio of the fraction of diffuse radiation scattered downward to that scattered upward by a scattering layer of optical thickness τ is shown in Fig. 3 for three incident directions. As one might expect, the case having the most (or least) forward-peaked phase function has consistently the highest (or lowest) ratio.

Figs. 4 and 5 show a similar consistency in that $S^{(0)}$ is lowest and $T^{(0)}$ highest, generally, for model 1 which

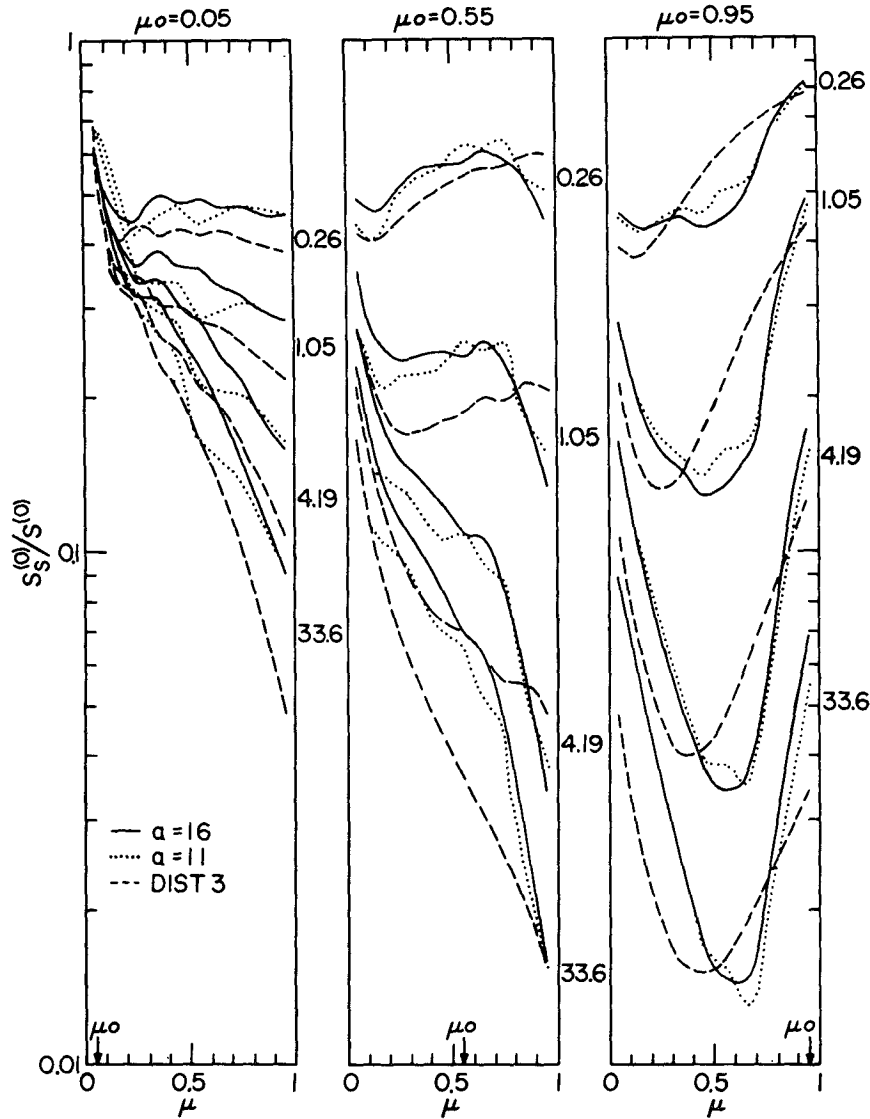


FIG. 6. The ratio of diffuse radiation reflected by a single scattering $S_s^{(0)}$ to that reflected by all orders of scattering $S^{(0)}$ vs μ for the three scattering models described in the legend to Fig. 1. Optical depth is indicated beside each set of curves.

has the most forward-peaked phase function. The sensitivity to phase function is strongly diminished when the optical depth becomes much greater than about 10. The consistent shapes of the curves for the greater optical depths ($\tau \geq 8$) show that the multiple scattering and integration over azimuth smooth out most detail introduced by the single scattering phase function.

Figs. 6 and 7 give the ratios of single scattering to multiple scattering for reflection and transmission, respectively. The variation in these ratios resulting from changes in phase function are less consistent than in the previous figures, although the differences are appreciable for certain values of μ , μ_0 and τ .

5. Conclusions

1) Changes in the single scattering phase function which result from slight changes in the size and/or index of refraction of the scattering particles cause considerable shifts in the absolute values of $S^{(0)}$ and $T^{(0)}$. The variation of these quantities with incident and emergent directions, i.e., the shapes of the curves, are approximately the same for all three cases studied. This discourages any inference of particle size or index of refraction from observations of $S^{(0)}$ and $T^{(0)}$, because in practice one does not know the optical depth of the cloud layer and therefore cannot assign absolute values to $S^{(0)}$ and $T^{(0)}$.

2) The results of the multiple-scattering calculations

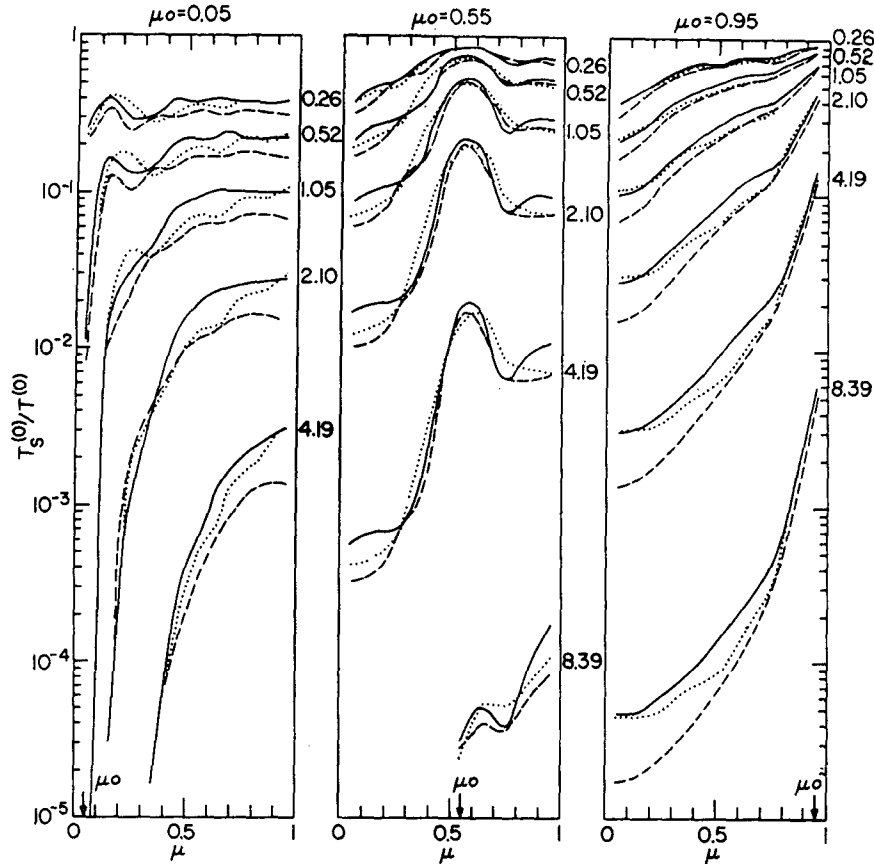


FIG. 7. The ratio of diffuse radiation transmitted by a single scattering $T_s^{(0)}$ to that transmitted by all orders of scattering $T^{(0)}$ vs μ for the three scattering models described in the legend of Fig. 1. Optical depth is indicated beside each set of curves.

presented in Twomey *et al.* (1966) are generally applicable for scattering layers for which the single-scattering phase function is not grossly different from that of spherical water droplets in the size range of 2–12 μ radius. This is especially true for optically thick clouds ($\tau \gg 10$).

REFERENCES

- Twomey, S., H. Jacobowitz and H. B. Howell, 1966: Matrix methods for multiple-scattering problems. *J. Atmos. Sci.*, **23**, 289–296.
- , —, and —, 1967: Light scattering by cloud layers. *J. Atmos. Sci.*, **24**, 70–79.